Energy Engineering

Tech Science Press

Doi:10.32604/ee.2025.065331

ARTICLE

Energy Recycling System for Harnessing Industrial Rotational Kinetic Energy

Md Tanjil Sarker[1,*], See Wei Jing[1], Gobbi Ramasamy[1,*], Siva Priya Thiagarajah[1] and Md. Golam Sadeque[2]

[1]Faculty of Engineering, Multimedia University, Cyberjaya, 63100, Malaysia
[2]Department of EEE, Pabna University of Science and Technology, Pabna, 6600, Bangladesh

*Corresponding Authors: Md Tanjil Sarker. Email: tanjilbu@gmail.com; Gobbi Ramasamy. Email: gobbi@mmu.edu.my

Received: 10 March 2025; Accepted: 18 April 2025; Published: 27 June 2025

ABSTRACT: Industrial processes often involve rotating machinery that generates substantial kinetic energy, much of which remains untapped. Harvesting rotational kinetic energy offers a promising solution to reduce energy waste and improve energy efficiency in industrial applications. This research investigates the potential of electromagnetic induction for harvesting rotational kinetic energy from industrial machinery. A comparative study was conducted between disk and cylinder-shaped rotational bodies to evaluate their energy efficiency under various load conditions. Experimental results demonstrated that the disk body exhibited higher energy efficiency, primarily due to lower mechanical losses compared to the cylinder body. A power management circuit was developed to regulate and store the harvested energy, integrating voltage, current, and speed sensors along with a charge controller for battery storage. The experimental setup successfully converted rotational kinetic energy into usable electrical power, with the disk achieving up to 16.33 J of recycled energy, outperforming the cylinder. The disk body demonstrated higher energy recovery efficiency compared to the cylinder, particularly under the 40 W resistive load condition. These findings demonstrate the feasibility of implementing energy recycling systems in industrial settings to enhance sustainability, reduce energy consumption, and minimize waste. Future research should focus on optimizing power management systems and improving energy harvesting efficiency to enable wider adoption of energy recycling technologies in various industrial applications.

KEYWORDS: Rotational kinetic energy; electromagnetic induction; energy harvesting; energy efficiency; mechanical loss; industrial energy recycling; sustainable energy solutions

1 Introduction

Electric motors are integral to industrial applications, accounting for a substantial share of global energy consumption [1]. Enhancing their energy efficiency is imperative for minimizing operational costs and reducing environmental impact. This research investigates the integration of energy storage systems with kinetic energy recycling methodologies to optimize energy efficiency in industrial motor-driven systems. A key focus is on the extraction of rotational kinetic energy from free-running mechanical loads, providing a framework for energy recovery through electromagnetic induction.

In Malaysia, the industrial sector is the largest energy consumer, with electric motors contributing significantly to overall energy demand [2]. While conventional energy-saving strategies, such as high-efficiency motors and variable speed drives (VSD), have been widely adopted to improve load factors, these approaches do not leverage the inherent kinetic energy available in industrial machinery [3]. Unlike the regenerative braking systems employed in electric vehicles to recover energy from deceleration, industrial

processes often dissipate rotational kinetic energy as waste. Existing studies suggest that energy recovery technologies can markedly enhance industrial energy efficiency [4]. This research investigates the feasibility of converting untapped rotational kinetic energy into electrical power for industrial applications.

This study is structured around three primary objectives:

1. Kinetic Energy Characterization: Analytical modeling quantifies available rotational kinetic energy using parameters such as moment of inertia, angular velocity, and torque.
2. Energy Harvesting via PMSG: A permanent magnet synchronous generator (PMSG) converts rotational kinetic energy into electrical power, with efficiency validated through comparative analysis of disk and cylinder configurations.
3. Power Management and Storage: A rectifier, DC-DC buck converter, and charge controller regulate and store the harvested energy in a battery for optimized industrial application.

The research methodology encompasses mathematical modeling, finite-element physics-based simulations, and experimental validation to optimize the extraction of kinetic energy from rotational machines. The study specifically focuses on two geometric configurations disk and cylindrical bodies to assess their respective energy conversion efficiencies under varying operational conditions.

The structure of this paper is as follows: Section 2 provides a comprehensive review of kinetic energy harvesting methodologies, with a focus on electromagnetic energy conversion from rotational bodies. Section 3 details the research methodology, encompassing analytical modeling, experimental setup, and power management system design. Section 4 presents the experimental results and key findings, highlighting comparative performance metrics. Finally, Section 5 concludes the study with insights into the practical implementation of industrial kinetic energy harvesting systems and outlines potential avenues for future research.

2 Background of the Study

The research on energy harvesting systems explores various methods to recover wasted energy in industrial settings. Wind-based energy harvesting techniques, such as wind turbines, vertical axis wind turbines (VAWT), and hybrid solar-flue gas chimneys, have demonstrated potential in capturing energy from exhaust gases and industrial airflow. However, challenges remain in integrating these systems with existing industrial processes, scaling up their implementation, and optimizing their efficiency [5]. Future work should focus on large-scale testing, improving environmental benefits, and enhancing system performance. Similarly, exhaust and waste energy utilization has been explored through exhaust air energy harvesting and small-scale wind turbines, with promising results in industrial applications. However, concerns regarding long-term durability and scalability need to be addressed through further research on system integration and performance optimization.

Energy recycling systems play a crucial role in sustainable industrial applications by capturing and repurposing energy that would otherwise be wasted [6]. These systems enhance overall energy efficiency while reducing environmental impact, particularly in industries where continuous machinery operation results in substantial energy losses. Among various energy recycling methods, rotational kinetic energy presents significant potential for electricity generation, especially in high-speed industrial processes [7]. Energy recycling can be categorized into thermal, mechanical, and electrical methods. Thermal recycling captures waste heat from industrial operations using heat exchangers, steam turbines, or organic Rankine cycles. Mechanical energy recycling focuses on kinetic energy conversion, such as regenerative braking in industrial machinery [8], while electrical energy recycling involves technologies like regenerative braking in electric vehicles to store and reintegrate power into the grid.

In industrial settings, rotational kinetic energy is widely available due to the constant operation of rotating machinery. Techniques similar to regenerative braking in electric vehicles can be applied to harvest this energy [9]. The primary components of such systems include energy harvesting mechanisms, such as flywheels and rotating disks, which store rotational energy, and generators that convert mechanical energy into electricity. Power management circuits regulate energy flow to ensure efficient storage and utilization. The energy harvesting process involves three key steps: capturing rotational energy from moving machinery [10], converting kinetic energy into mechanical and then electrical power, and storing or utilizing the generated electricity in batteries or feeding it into the grid.

Several case studies have demonstrated the effectiveness of energy recycling systems in industrial environments. Factories using large rotating machinery have successfully integrated energy recycling technologies, achieving notable energy savings and cost reductions [11]. Similarly, regenerative braking in electric and hybrid vehicles has proven to be a highly efficient energy recovery mechanism, significantly improving system efficiency [12]. The potential for rotational kinetic energy utilization in industrial settings is vast, with the adoption of advanced energy recycling systems enabling industries to enhance energy efficiency while minimizing environmental impact. Continued research is necessary to refine these technologies, optimize power management, and expand practical applications to maximize energy recovery [13].

Regenerative braking systems in industrial motors capture energy during braking and convert it back into electrical power, reducing energy consumption and improving efficiency. These systems can lead to significant energy savings, especially in industries with heavy machinery that frequently decelerates, such as in manufacturing and material handling. Studies have shown potential energy savings of up to 20%–30% [1]. However, challenges remain in integrating these systems with legacy equipment, particularly in terms of compatibility and control optimization [14]. Future advancements should focus on improving energy conversion efficiency and seamless integration with existing industrial systems. Current energy recovery systems in industrial applications, such as regenerative braking and mechanical energy harvesting, have demonstrated substantial potential for improving energy efficiency [15]. However, these systems encounter several limitations, particularly in terms of energy conversion efficiency and integration with legacy systems [16]. Many existing recovery systems exhibit suboptimal energy conversion rates, especially when faced with irregular operational conditions such as fluctuating loads or variable speeds, which hinder their effectiveness [17]. Additionally, the integration of modern energy recovery technologies with legacy industrial systems presents significant challenges [18]. Older machinery, which often lacks the necessary control mechanisms or interfaces, is incompatible with advanced recovery systems, limiting the applicability of these technologies in established industrial environments. To address these challenges, future research should focus on improving the conversion efficiency of energy recovery systems and developing universal integration solutions that facilitate the adoption of these systems across a wide range of industrial applications. Mechanical intelligent energy harvesting addresses key challenges such as poor output, low adaptability, and reliability in AIoT systems. By enabling autonomous response to external stimuli, it optimizes energy harvesting without the need for central controllers, thus improving efficiency and contributing to net-zero emissions for AIoT power supplies [19]. An example of this technology is the DCIS-floor, which uses triboelectric nanogenerators (TENGs) to capture mechanical energy from pressure and shear forces created by human movement [20]. This self-powered system converts kinetic energy into electrical power, ensuring functionality without external energy sources and enhancing the sustainability and reliability of smart floors in future smart buildings.

In the context of renewable energy, Maximum Power Point Tracking (MPPT) algorithms play a vital role in optimizing energy extraction from solar modules by ensuring power delivery remains at the maximum point on the P-V characteristic curve. These controllers continuously monitor output current and voltage, adjusting the converter's duty cycle to match source impedance with the load. However, challenges persist in accurately tracking voltage fluctuations and optimizing control signals for maximum power output. Research is ongoing to improve the efficiency of MPPT algorithms, particularly the Perturb and Observe (P&O) method, which is widely used for its cost-effectiveness [21]. Further advancements in step-size selection and algorithm simplification could lower MPPT production costs, making solar energy systems more accessible [22].

Permanent magnet speed regulators offer an efficient means of torque transmission and speed regulation in industrial applications [23]. These regulators operate through magnetic coupling between the guide and permanent magnets, enabling precise speed control and reducing energy consumption. Their key advantages include over 95% transmission efficiency, a soft start mechanism that minimizes mechanical wear, and broad applications in pumps, fans, centrifugal loads, and conveyors. In wind energy systems, a double magnet coupling mechanism has been proposed to enhance wind speed adaptability and improve power output. Experimental studies have demonstrated that symmetrical opposite magnet arrangements can reduce startup torque and increase efficiency, achieving a maximum average power of 22.2 mW. These findings highlight the relevance of permanent magnetic coupling in applications such as non-contact braking, vibration absorption, and cogging torque reduction in wind turbines and electric motors [24]. Table 1 shows the Research Findings for Energy Harvesting Systems.

Table 1: Research findings for energy harvesting systems

Aspect	Research summary	Research gaps	Contribution of this research	Ref.
Hybrid energy harvesting	Recent research combines piezoelectric, triboelectric, and electromagnetic mechanisms.	Limited efficiency in low-frequency rotational environments.	Proposed an ultra-low-frequency rotational harvester using frequency up-conversion.	[25]
Low-speed direct-drive generators	Low-speed PMSGs have been evaluated for marine and industrial current energy harvesting.	High AC-DC conversion loss at low speeds.	Optimized load resistance to improve efficiency in low-RPM scenarios.	[26]
Wind energy harvesting	Hybrid nanogenerators have been designed for ambient wind capture using rotary structures.	Environmental variations limit harvesting consistency.	Enhanced magnetic and friction layer design for higher and stable output.	[27]

(Continued)

Table 1 (continued)

Aspect	Research summary	Research gaps	Contribution of this research	Ref.
Water flow energy harvesting	Rotating hybrid piezoelectric-electromagnetic systems tested in underwater flows.	Power output remains modest for real-world loads.	Developed structure yielding 21% improvement over standalone harvesters.	[28]
Orientation-adaptive harvesters	EM harvesters designed to adapt to directional wind-induced vibrations.	Most systems have fixed structure; limited directional adaptability.	Introduced rotatable bluff body increasing average power output significantly.	[29]

Overall, energy recycling systems offer transformative opportunities for industries to improve energy efficiency and sustainability. By harnessing rotational kinetic energy, industries can recover wasted energy and convert it into usable electricity. The integration of MPPT optimization in renewable energy systems and permanent magnet speed regulators further supports energy conservation efforts across multiple applications [30]. Future research should focus on refining energy harvesting mechanisms, optimizing MPPT algorithms, and expanding the use of magnetic coupling technologies to maximize efficiency and cost-effectiveness in sustainable energy systems [31].

3 Research Methodology

In this research, two different heavy mass bodies, disk and cylinder, were chosen. The disk body was defined as a simple model, whereas the Cylinder body was defined as a complex model. In this way, the difference in the mechanical part can be evaluated quantitatively. Fig. 1 illustrates the systematic framework adopted for this study to analyze, harvest, and manage rotational kinetic energy from disk and cylinder bodies. The methodology begins with the kinetic energy characterization phase, where analytical modeling is used to determine the moment of inertia, angular velocity, and torque for both geometries. This phase establishes the theoretical foundation for calculating the available rotational kinetic energy. The subsequent phase, energy harvesting via Permanent Magnet Synchronous Generator (PMSG), involves the conversion of rotational kinetic energy into electrical power. The efficiency of this conversion is evaluated based on the comparative analysis of the disk and cylinder configurations under varying load conditions.

Following energy conversion, the power management and storage system is designed to regulate the harvested electrical energy. This involves the use of a rectifier for AC-to-DC conversion, followed by a DC-DC buck converter that steps down the voltage to appropriate levels for battery charging. A charge controller ensures the battery is optimally charged, enabling efficient storage and retrieval of the harvested energy. The experimental setup integrates voltage, current, and speed sensors, with the data processed by a microcontroller that manages the power flow and switching between the utility grid and the battery. The structured approach ensures that each step is meticulously linked, beginning from the theoretical analysis of rotational kinetic energy and progressing through experimental validation and optimization of the energy harvesting system. This methodology facilitates the comparison of energy conversion efficiencies between

the disk and cylinder bodies and provides a comprehensive framework for the development of effective power management strategies in industrial energy recycling application.

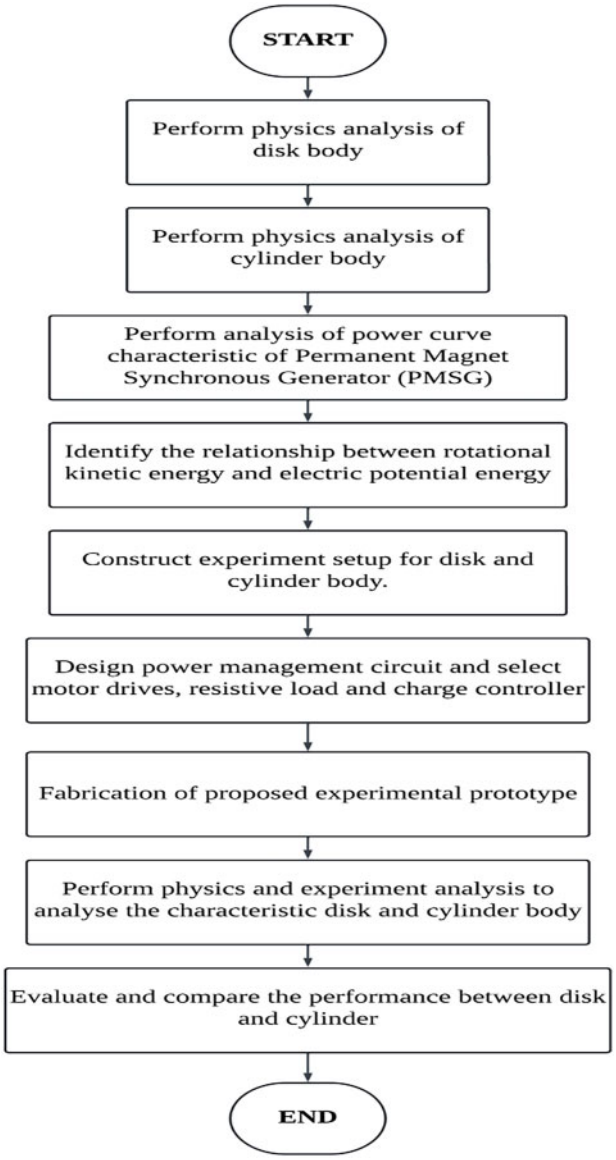

Figure 1: Process flow of research methodology

3.1 Energy Harvesting and Power Management System

Fig. 2 illustrates the structural layout of the energy harvesting system, highlighting the interaction between its components. The Primary System includes a motor, powered by either the utility grid or a battery, which drives a heavy mass body (disk/cylinder) that accumulates rotational kinetic energy. The system integrates voltage, current, and Hall effect sensors to monitor the electrical parameters. A microcontroller processes the sensor data and autonomously switches the power source between the utility grid and battery via solid-state relays (SSRs). The generated mechanical energy from the mass body is converted into electrical

power by a permanent magnet synchronous generator (PMSG), which is then rectified by a full-bridge rectifier, converting AC into DC. The rectified DC power is transferred to the Secondary System for regulation and storage. The Secondary System consists of a DC-DC buck converter that steps down the voltage to appropriate levels for battery charging. The energy is stored in the battery and can be released for use when required, ensuring continuous power delivery to the load.

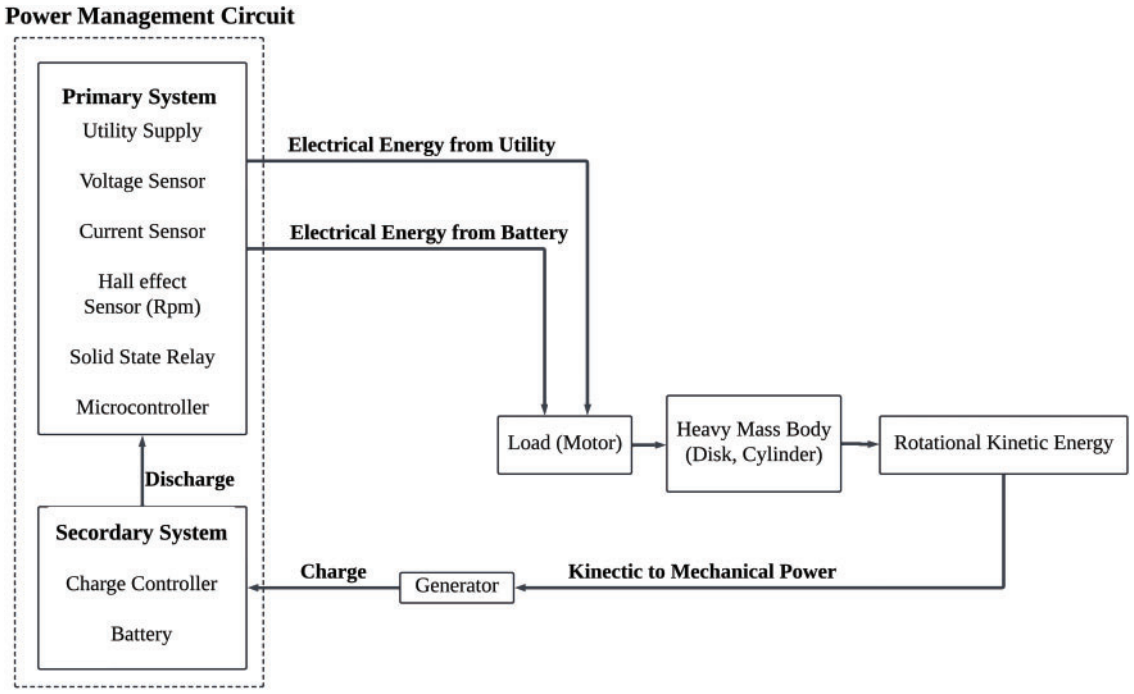

Figure 2: Block diagram of energy harvesting system

Fig. 3 presents a schematic of the power management circuit, showing the interaction between the Primary and Secondary Systems for efficient energy harvesting and storage. The Primary System comprises a utility supply, motor, and heavy mass body, which together facilitate the conversion of rotational kinetic energy into electrical energy. Sensors for voltage, current, and rotational speed (via Hall effect) continuously monitor system parameters. The microcontroller processes this data and uses SSRs to control the power switching between the utility grid and the battery, ensuring optimized energy flow. The electrical output from the generator is rectified by a full-bridge rectifier to convert the AC output to DC. This DC power is then fed into the Secondary System, where a DC-DC buck converter regulates the voltage and current for efficient battery charging. The charge controller ensures the battery charging/discharging process is optimized for energy storage and retrieval, reducing dependency on the utility grid while maintaining a stable power supply to the load. By controlling the amount of energy harvested and ensuring that it is stored efficiently, the charge controller minimizes the abrupt energy dissipation, leading to a more gradual and steady decrease in rotational speed. This controlled energy transfer helps maintain a consistent deceleration rate, which is less influenced by mechanical losses compared to other load conditions

3.2 Design of the Energy Harvesting System

The experimental setup depicted in the Fig. 4 represents a comprehensive energy harvesting system designed to convert rotational kinetic energy into electrical energy. The system comprises a DC power supply,

DC brushed motor, flywheel, Permanent Magnet Synchronous Generator (PMSG), motor driver, resistive load, and controller. The DC power supply delivers electrical energy to the DC brushed motor, initiating rotational motion in the flywheel, which functions as an energy storage device to maintain rotational inertia. This kinetic energy is subsequently transferred to the PMSG, which facilitates electromechanical energy conversion, generating electrical power.

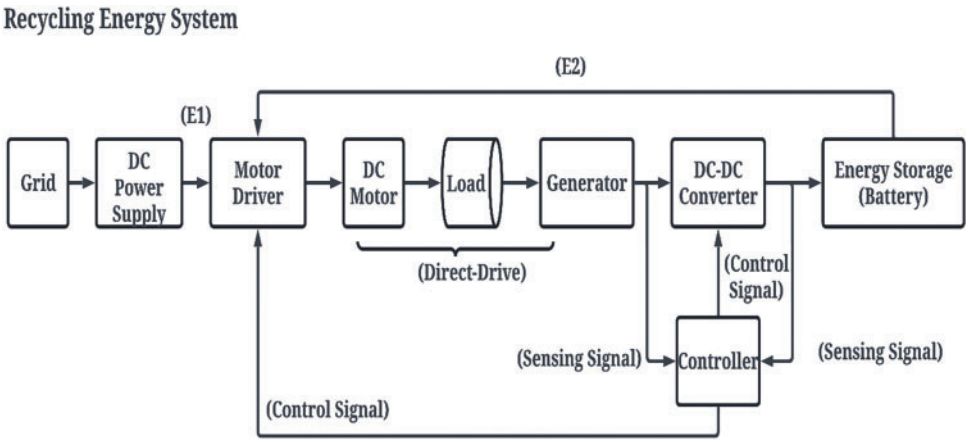

Figure 3: Schematic of the proposed power management circuit for recycling energy system

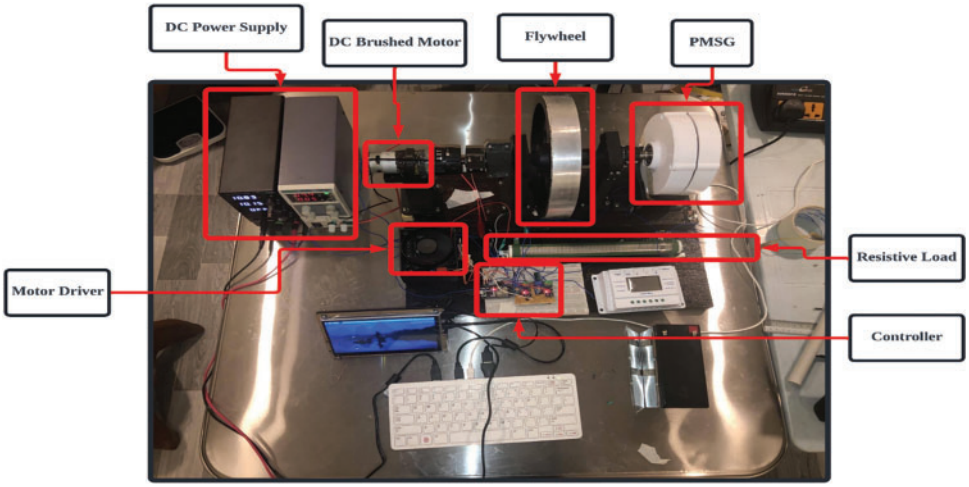

Figure 4: Outlook of the prototype for the disk body

A motor driver is employed to regulate the motor's operational parameters, ensuring precise control over speed and torque. The harvested electrical energy is then directed to a resistive load, serving as a controlled energy dissipation mechanism to evaluate system performance under various conditions. The controller plays a crucial role in optimizing system efficiency by managing power flow, load regulation, and performance monitoring. This experimental prototype is instrumental in assessing the feasibility of rotational kinetic energy recovery, with potential applications in sustainable energy systems, industrial energy recycling, and smart grid integration. The setup enables a detailed analysis of energy conversion

efficiency, providing insights into the optimization of mechanical-to-electrical energy transformation for enhanced energy utilization.

3.3 Theory for Energy Harvesting

Energy harvesting, also known as energy scavenging, is the process of capturing small amounts of ambient or wasted energy from the environment and converting it into usable electrical power. This energy can come from various sources such as mechanical vibrations, temperature gradients, solar radiation, electromagnetic waves, and kinetic energy. Table 2 presents the key mathematical equations used to estimate rotational kinetic energy, mechanical losses, and harvested energy. These equations are essential for quantifying the energy available for harvesting, calculating energy losses due to friction and deformation, and determining the efficiency of the energy conversion process. The estimated available rotational kinetic energy is calculated based on the moment of inertia and angular velocity, while mechanical losses are quantified to understand energy dissipation during harvesting. The harvested energy percentage reflects the system's efficiency, directly linking the theoretical model to the experimental results, as discussed in the results sections of the study.

Table 2: The mathematical theory for energy harvesting [32]

Physical aspect	Equation	Explanation
Estimated available rotational kinetic energy, J (Ws)	$E_w = \frac{1}{2} * J * w^2$	E_w = Estimated available rotational kinetic energy, J (Ws) J = Moment of Inertia, kgm^2 w = Angular Velocity, rad/s
Estimated capacitance, F	$C = \frac{E_c * 2}{V^2}$	C = Capacitor Capacitance [Farad] E_c =Energy in a Capacitor [J] V = Generated Voltage by PSMG [V]
Time constant, free running without harvesting conditions, s	$T_0 = \frac{Jn^2}{\alpha P_i}$	J is the moment of inertia [kgm^2] n is the initial speed of the motor when braking starts [rpm] P_i is the initial power delivered by the motor to the braking resistor [W] α is a constant value
Input mechanical power, $\boldsymbol{P_m}$ [W]	$P_{mech} = T_m \times W = (k + l + j) \times W$	T_m [Nm] is the mechanical torque k value is a constant value to overcome the force of gravity acting on the left side to keep the disk rotating in a clockwise direction [Nm] l are the lump sum mechanical losses friction [Nm]. j is the loss due to the deformation and adhesion between the contact surface [Nm] w = Angular Velocity, rad/s
Mechanical loss, $\boldsymbol{P_l}$ [W]	$P_l = (k + l + j) \times W$	k value is a constant value to overcome the force of gravity acting on the left side to keep the disk rotating in a clockwise direction [Nm]

(Continued)

Table 2 (continued)

Physical aspect	Equation	Explanation
		l are the lump sum mechanical losses friction [Nm]. j is the loss due to the deformation and adhesion between the contact surfac [Nm] w = Angular Velocity of the rotating object, rad/s
Output power (Pout), W	$P_g = \frac{V^2}{R} = I^2R$	V is the generated voltage by PMSG [V] R is the load resistance [Ω]
Energy loss in friction (%)	$\eta_l = \frac{P_l}{P_m} \times 100\%$	P_l = Mechanical Loss [W] P_m = Input Mechanical Power [W]
Harvested energy (%)	$\eta_H = \frac{P_g}{P_m} \times 100\%$	P_g = Output Power [W] P_m = Input Mechanical Power [W]

4 Results and Discussion

This section presents the results obtained from the experimental analysis, focusing on the measurement of harvested electrical energy from both disk and cylinder bodies under various load conditions. The analysis aims to compare the theoretical and experimental recycling energies, evaluate the efficiency of energy recovery, and identify the practical inefficiencies that impact the overall performance of the energy recycling systems.

4.1 Experimental Analysis of Disk Body

The speed-time curves in Fig. 5 provide additional insight into the dynamic behavior of the disk body under different conditions. The free-running curve shows a gradual decline in speed, while the 40 W load and 20 W load conditions exhibit steeper declines, reflecting the energy dissipation in these systems. The curve for the 20 W charge controller shows a more controlled descent compared to the 40 W load, indicating a more gradual energy dissipation due to the presence of the charge controller.

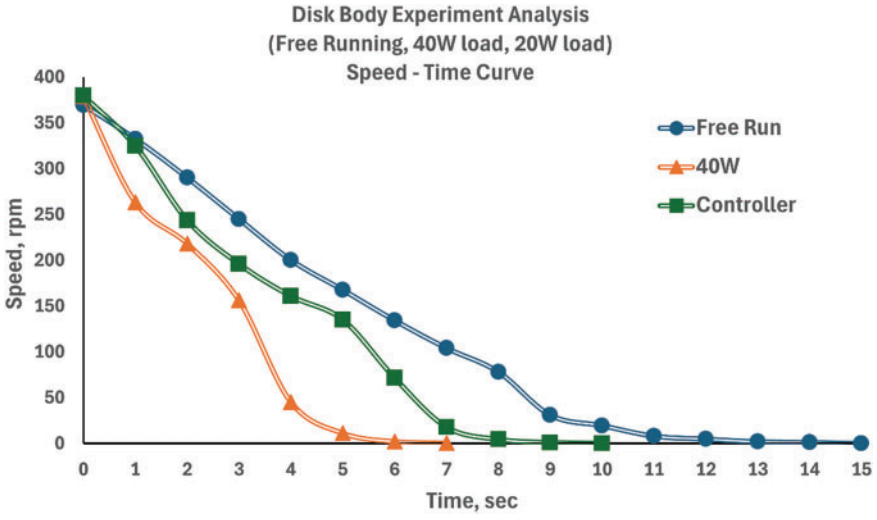

Figure 5: Speed-time curves for disk body under different load conditions

The results from Table 3 present a comparison of output power from a disk body under various speed conditions, detailing the voltage and output power for three scenarios: free running, 40 W resistive load, and 20 W charge controller. The data highlights that the free-running condition consistently shows zero output power across all speeds, as expected due to the absence of a load. For the 40 W resistive load, the output power is highest at 375 rpm and decreases significantly with the reduction in speed, illustrating the reliance on higher speeds for efficient energy generation. The 20 W charge controller scenario shows a regulated power output, with a more controlled decrease in power as speed diminishes. The voltage readings align with the output power trends, indicating a direct relationship between kinetic energy and electrical output in the disk body system.

The results presented in Table 4 compare the harvested energy from a disk body under three conditions: free running, 40 W resistive load, and 20 W charge controller. In the free-running condition, all mechanical power (17.1 W) is lost to friction, resulting in zero output power and no harvested energy, indicating complete energy dissipation without an external load. For the 40 W resistive load, the mechanical power input is 57.1 W, with a continuous power loss of 17.1 W due to friction, representing the ongoing energy dissipation as the rotating body slows down over time. This loss occurs continuously during the operation of the system, reflecting the frictional forces that oppose the rotation, resulting in an output power of 40 W. This condition shows an energy loss in friction of 30% and a harvested energy of 70%, demonstrating significant energy recovery despite the frictional losses. Under the 20 W charge controller condition, the mechanical power input is 37 W, with the same frictional power loss of 17.1 W, yielding an output power of 20 W. Here, the energy loss in friction increases to 46.22%, and the harvested energy is 53.78%. Although the harvested energy is lower compared to the 40 W resistive load condition, the system still manages to recover more than half of the input energy.

Table 3: Comparison of output power from disk body under various speed conditions

Speed, w [rpm]	Voltage generated by PMSG [V]	Output power, W (Measured)		
		Free running	40 W resistive load	20 W charge controller
375	24.00	0	44.30	20
300	19.30	0	17.39	13.93
200	12.73	0	1.48	0
100	6.47	0	0	0

Table 4: Comparison of harvested energy from disk body through experiment

Number	Condition	Input mechanical power, P_m [W]	Mechanical loss, P_l [W]	Output power (Pout), W	Energy loss in friction (%)	Harvested energy (%)
1	Free running	17.1	17.1	0	100.00	0
2	40 W resistive load	57.1	17.1	40	30.00	70.00
3	20 W charge controller	37.1	17.1	20	46.22	53.78

The results in Table 5 illustrate the energy efficiency of a disk body through experimentation, focusing on the rotational kinetic energy and the corresponding recycling energy under three conditions. The disk body's rotational kinetic energy is measured at 23.33 joules (J). In the free-running condition, no energy is recycled, indicating that without an external load, the kinetic energy of the system is entirely dissipated without being converted into usable energy. In contrast, the 40 W resistive load condition achieves a recycling energy of 16.33 J, the highest among the tested conditions and demonstrates that the resistive load effectively converts a significant portion of the rotational kinetic energy into usable energy, highlighting its efficiency in energy recovery applications. The 20 W charge controller condition yields a recycling energy of 12.55 J, which, while lower than the 40 W resistive load, is still substantial. The results proved that the charge controller is also effective in harvesting energy, though with slightly lower efficiency compared to the resistive load.

Table 5: Energy efficiency through experiment from disk body

Rotational kinetic energy, J = 23.33 J	Free running	40 W resistive load	20 W charge controller
Recycling energy, J	0	16.33	12.55

4.2 Experimental Analysis of Cylinder Body

Fig. 6 illustrates the speed-time curves for a cylinder body under three conditions: free running, 40 W load, and 20 W charge controller. The graph reveals how the speed of the cylinder body, measured in revolutions per minute (rpm), decreases over time in seconds for each condition. In the free-running condition, the speed gradually decreases from approximately 380 rpm to zero over 10 s, showing a steady and continuous decline due to the absence of external loads, with deceleration primarily driven by internal frictional forces. For the 40 W load condition, the speed drops sharply from about 380 rpm to zero in around 4 s. This steep decline indicates significant energy dissipation caused by the high resistive load, which quickly reduces the cylinder's rotational speed. The rapid deceleration suggests that the 40 W resistive load imposes a substantial drag force, converting much of the rotational kinetic energy into other forms of energy, likely heat.

In contrast, the 20 W charge controller condition shows a more moderate rate of deceleration, with the speed decreasing from around 380 rpm to zero in about 6 s. This curve demonstrates a more controlled and gradual deceleration compared to the 40 W load, indicating an efficient energy conversion process that moderates the speed reduction. The 20 W charge controller effectively manages the conversion of kinetic energy into electrical energy, maintaining a steady reduction in rotational speed.

Table 6 compares the output power from a cylinder body under various speed conditions, illustrating the voltage and output power for three scenarios: free running, 40 W resistive load, and 20 W charge controller. At a speed of 375 rpm, the voltage is 24.00 V, with the output power reaching 40.00 W under the 40 W resistive load and 20.00 W with the 20 W charge controller, while the free-running condition yields no output power. As the speed decreases to 300 rpm, the voltage drops to 19.30 V, and the output power reduces to 17.39 W for the 40 W resistive load and 13.93 W for the 20 W charge controller, with the free-running condition still showing no output power. At 200 rpm, the voltage further declines to 12.73 V, with output power diminishing to 0.83 W under the 40 W resistive load and zero output for both the free-running condition and the 20 W charge controller. Finally, at the lowest speed of 100 rpm, the voltage is 6.47 V, and all conditions show zero output power.

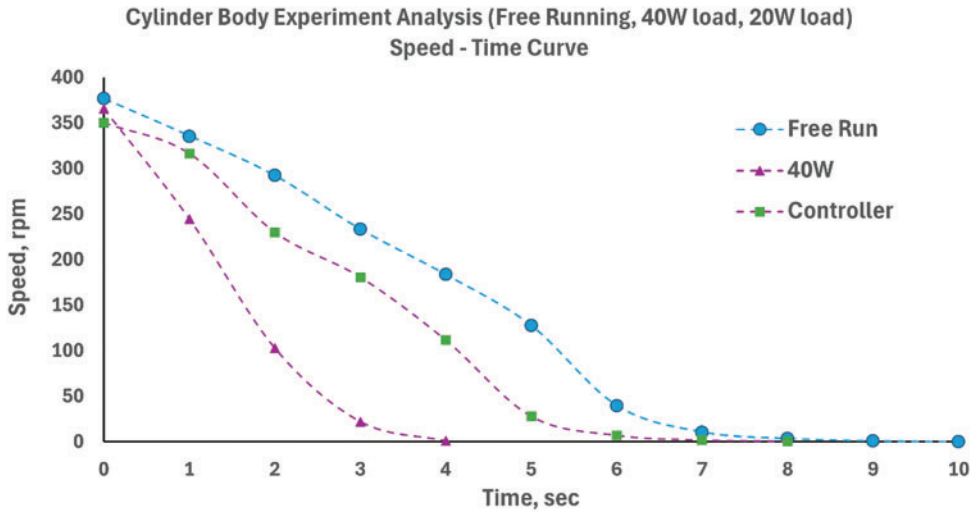

Figure 6: Speed-time curves for cylinder body under different load conditions

Table 6: Comparison of output power from cylinder body under various speed conditions

Speed, rpm	Voltage	Output power, W		
		Free running	40 W resistive load	20 W charge controller
375	24.00	0	40.00	20.00
300	19.30	0	17.39	13.93
200	12.73	0	0.83	0
100	6.47	0	0	0

Table 7 compares the harvested energy from a cylinder body under three conditions: free running, 40 W resistive load, and 20 W charge controller. The data includes measurements of mechanical power (Pd), power loss (Pl), output power (Pout), energy loss in friction, and the percentage of harvested energy. In the free-running condition, the mechanical power of 46.68 W is entirely lost to friction, resulting in zero output power and no harvested energy, indicating complete energy dissipation without an external load. Under the 40 W resistive load condition, the system experiences a mechanical power input of 86.68 W, with 46.68 W lost to friction, yielding an output power of 40.00 W. This condition shows an energy loss in friction of 53.85% and a harvested energy percentage of 46.15%, demonstrating significant energy recovery despite the frictional losses. For the 20 W charge controller condition, the mechanical power input is 66.68 W, with the same frictional power loss of 46.68 W, resulting in an output power of 20.00 W. The energy loss in friction increases to 70.01%, and the harvested energy percentage is 29.99%, which, although lower than the 40 W resistive load condition, still indicates substantial energy recovery.

Table 8 shows a comparison of energy efficiency based on tests done on a cylinder body. In three different situations, the tests looked at the rotational kinetic energy and the recycling energy that came from it: free running, 40 W resistive load, and 20 W charge controller. The rotational kinetic energy is measured at 33.63 joules (J). Without an external load, the system does not convert the rotational kinetic energy into usable energy in the free-running condition. Under the 40 W resistive load condition, the system achieves a recycling energy of 15.52 J, the highest among the tested conditions. The results showed that the resistive load is effective in converting a significant portion of the rotational kinetic energy into usable energy, highlighting

its efficiency in energy recovery applications. The 20 W charge controller produces 10.08 J of recycling energy. Although this is lower than the 40 W resistive load, it still demonstrates substantial energy recovery. The difference in recycling energy between the two loaded conditions may be due to the varying mechanisms of energy conversion and the inherent losses in each system.

Table 7: Comparison of harvested energy from cylinder body through experiment

No	Condition	Input mechanical power, P_m [W]	Mechanical loss, P_l [W]	Output power (Pout), W	Energy loss in friction (%)	Harvested energy (%)
1	Free running	46.68	46.68	0.00	100.00	0.00
2	40 W resistive load	86.68	46.68	40.00	53.85	46.15
3	20 W charge controller	66.68	46.68	20.00	70.01	29.99

Table 8: Energy efficiency through experiment from cylinder body

Rotational kinetic energy, J = 33.63 J	Free running	40 W resistive load	20 W charge controller
Recycling energy, J	0	15.52	10.08

4.3 Comparison between Experimental Analysis between of Disk and Cylinder Body

Table 9 presents a detailed comparison of the experimental analysis between a disk body and a cylinder body, highlighting various physical aspects such as mass, radius, moment of inertia, rotational kinetic energy, mechanical loss, and recycling energy under different conditions. The disk has a mass of 5 kg and a radius of 0.11 m, while the cylinder has a mass of 15 kg and a radius of 0.076 m. The moment of inertia is 0.030 kg m^2 for the disk and 0.044 kg m^2 for the cylinder. The rotational kinetic energy is measured at 27.45 joules (J) for the disk and 33.25 J for the cylinder. Mechanical losses are significantly different, with the disk experiencing 17.1 W (W) of loss compared to the cylinder's 46.68 W. In the free-running condition, neither the disk nor the cylinder recycles any energy, both showing 0 J. Under the 40 W resistive load condition, the disk recycles 16.33 J of energy, slightly higher than the cylinder's 15.52 J. The results indicate that the disk is more efficient in converting rotational kinetic energy into usable energy under this load condition. For the 20 W charge controller condition, the disk shows a recycling energy of 15.55 J, while the cylinder records 10.08 J. The results further underscore the disk's superior efficiency in energy recovery compared to the cylinder under these specific conditions.

Fig. 7 presents the actual speed-time curves for both disk and cylinder bodies under three different conditions: free running, 40 W load, and 20 W charge controller. The graph illustrates how the speed of the disk and cylinder bodies, measured in revolutions per minute (rpm), decreases over time in seconds for each condition. For the disk body, the speed gradually decreases from approximately 375 rpm to zero for 15 s in the free-running condition. This steady decline indicates minimal external forces acting on the system, with deceleration primarily due to internal frictional forces. Under the 40 W load condition, the disk's speed drops more sharply from around 375 rpm to zero in about 7 s, demonstrating significant energy dissipation due to the high resistive load. The 20 W charge controller condition shows a more controlled and gradual deceleration, with the speed decreasing from around 375 rpm to zero in approximately 10 s, indicating a more efficient energy conversion process that moderates the speed reduction.

Table 9: Comparison of experimental analysis between physics analysis of disk and cylinder body

Physics aspect	Disk	Cylinder
Mass, $\boldsymbol{m}$ k[g]	5	15
Radius, R [m]	0.11	0.076
Moment of Inertia, $\boldsymbol{J}$ [kg$\mathbf{m}^2$]	0.030	0.044
Rotational Kinetic Energy [J]	27.45	33.25
Mechanical Loss, $\boldsymbol{P_l}$ [W]	17.1	46.68
Recycling Energy [J]—Free Running	0	0
Recycling Energy [J]—40 W Resistive Load	16.33	15.52
Recycling Energy [J]—20 W Charge Controller	15.55	10.08

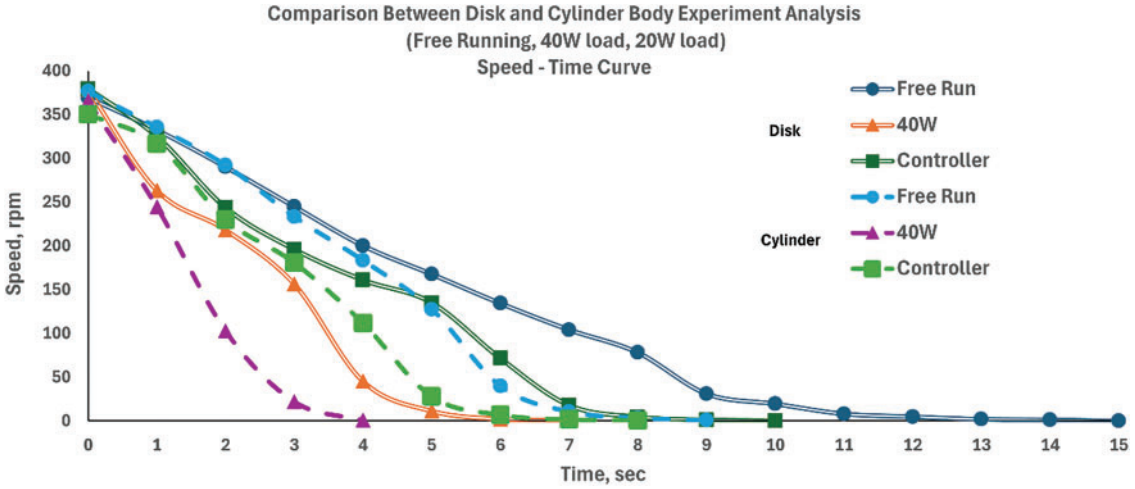

Figure 7: Comparative speed-time curves for disk and cylinder bodies under varying load conditions

For the cylinder body, the speed decreases from around 400 rpm to zero over 14 s in the free-running condition, similar to the disk. Under the 40 W load condition, the cylinder's speed drops sharply from around 400 rpm to zero in about 4 s, indicating substantial energy dissipation due to the high resistive load, which quickly reduces the cylinder's rotational speed. The 20 W charge controller condition shows a controlled deceleration from around 400 rpm to zero in about 8 s, reflecting a balanced energy conversion process. The comparison between the disk and cylinder bodies highlights their different deceleration rates under various conditions. The disk shows a more gradual decline in speed under the 20 W charge controller condition, suggesting more efficient energy harvesting compared to the cylinder. Under the 40 W load condition, both bodies exhibit rapid deceleration, but the disk maintains a slightly slower rate of decline, indicating less energy dissipation compared to the cylinder.

4.4 Comparison of Result Related to Physics and Experiment Analysis

The comparison of recycling energy between theoretical and experimental results for both disk and cylinder bodies reveals varying degrees of accuracy. The theoretical physics results are taken from [27]. As shown in Table 10, the disk body under free-running conditions showed no difference (0%), confirming the model's validity in no-load scenarios. For the 40 W resistive load, the theoretical value was 15.55 J, while the experimental result was 16.33 J, yielding a −4.89% difference. Under the 20 W charge controller condition,

the theoretical and experimental values were 13.73 and 12.55 J, respectively, resulting in an 8.98% difference. All differences remained within 10%, indicating reliable theoretical estimations for the disk body.

Table 10: Comparison of recycling energy between physics and experiment from disk body

Number	Condition	Recycling energy, J		Percentage differences (%)
		Physics result, J	Experiment result, J	
1	Free Running	0	0	0
2	40 W Resistive Load	15.55	16.33	−4.89
3	20 W Charge Controller	13.73	12.55	8.98

In Table 11, for the cylinder body, both theoretical and experimental results again matched under free-running conditions (0%). However, greater discrepancies were observed under load. At 40 W resistive load, theoretical recycling energy was 17.27 vs. 15.52 J experimentally, with a 10.67% difference. Under the 20 W charge controller condition, the theoretical value was 11.67 J compared to 10.08 J experimentally, showing a 14.62% difference. These results suggest that while theoretical predictions are reasonable, the cylinder body exhibits higher deviations, with percentage differences ranging from 10% to 15%, indicating a need for model refinement.

Table 11: Energy efficiency through experiment from cylinder body

Number	Condition	Recycling energy, J		Percentage differences (%)
		Physics result, J	Experiment result, J	
1	Free Running	0	0	0
2	40 W Resistive Load	17.27	15.52	10.67
3	20 W Charge Controller	11.67	10.08	14.62

5 Conclusion

This study investigated the feasibility of recycling untapped rotational kinetic energy from disk and cylinder bodies under various load conditions. The key findings are summarized as follows:

i. The disk body demonstrated higher energy recovery efficiency compared to the cylinder, particularly under the 40 W resistive load condition.
ii. The experimental recycling energy for the disk was 16.33 J, closely matching the theoretical value of 15.55 J, with a percentage difference of −4.89%.
iii. In contrast, the cylinder showed a theoretical value of 17.27 J and an experimental result of 15.52 J, resulting in a larger percentage difference of 10.67%.
iv. These discrepancies highlight that theoretical models may not fully account for practical inefficiencies such as heat loss, friction, and resistance variability.
v. The findings emphasize the importance of integrating real-world loss factors into the design of energy recycling systems.

Future research should focus on conducting long-term performance evaluations, optimizing energy recovery mechanisms, and enhancing system reliability and safety. Addressing these aspects will contribute to more efficient, sustainable, and impactful applications of energy recycling technologies in industrial systems.

Acknowledgement: The authors would like to express their heartfelt gratitude to Multimedia University, Malaysia, for their invaluable support throughout this journey. Their generous financial backing, access to state-of-the-art laboratory facilities, and seamless logistical assistance have been instrumental in bringing this research to fruition.

Funding Statement: The APC was funded by Research Management Centre, Multimedia University, Malaysia.

Author Contributions: Conceptualization, Md Tanjil Sarker, See Wei Jing and Gobbi Ramasamy; Methodology, Md Tanjil Sarker, See Wei Jing and Gobbi Ramasamy; Validation, Md Tanjil Sarker and See Wei Jing; Formal analysis, Md Tanjil Sarker and See Wei Jing; Investigation, Md Tanjil Sarker, See Wei Jing, Gobbi Ramasamy, Siva Priya Thiagarajah and Md. Golam Sadeque; Data curation, Md Tanjil Sarker and Gobbi Ramasamy; Writing—original draft, Md Tanjil Sarker and See Wei Jing; Writing—review & editing, Md Tanjil Sarker, See Wei Jing, Gobbi Ramasamy, Siva Priya Thiagarajah and Md. Golam Sadeque; Visualization, Md Tanjil Sarker, Md. Golam Sadeque and Gobbi Ramasamy; Supervision, Md Tanjil Sarker, Gobbi Ramasamy and Siva Priya Thiagarajah; Funding acquisition, Gobbi Ramasamy. All authors reviewed the results and approved the final version of the manuscript.

Availability of Data and Materials: The data that support the findings of this study are available from the corresponding author, (G. R.), upon reasonable request.

Ethics Approval: Not applicable.

Conflicts of Interest: The authors declare no conflicts of interest to report regarding the present study.

References

1. Saidur R. A review on electrical motors energy use and energy savings. Renew Sustain Energy Rev. 2010;14(3):877–98. doi:10.1016/j.rser.2009.10.018.
2. Shern SJ, Sarker MT, Ramasamy G, Thiagarajah SP, Al Farid F, Suganthi ST. Artificial Intelligence-based electric vehicle smart charging system in Malaysia. World Electr Veh J. 2024;15(10):440. doi:10.3390/wevj15100440.
3. Rajnath YK, Tiwari S, Kumar V. Thermodynamics for mechatronics. Comput Intell Tech Mechatron. 2024;8:41–81. doi:10.1002/9781394175437.ch2.
4. Zhang Q, Zhao X, Lu H, Ni T, Li Y. Waste energy recovery and energy efficiency improvement in China's iron and steel industry. Appl Energy. 2017;191:502–20. doi:10.1016/j.apenergy.2017.01.072.
5. Sisinni E, Saifullah A, Han S, Jennehag U, Gidlund M. Industrial internet of things: challenges, opportunities, and directions. IEEE Trans Ind Inform. 2018;14(11):4724–34. doi:10.1109/tii.2018.2852491.
6. Srivastava A, Pandey S, Shahwal R, Sur A. Recycling of waste into useful materials and their energy applications. In: Kandasamy S, Shah MP, Subbiah K, Manickam N, editors. Microbial niche nexus sustaining environmental biological wastewater and water-energy-environment nexus. Cham, Switzerland: Springer Nature; 2025. p. 251–96. doi: 10.1007/978-3-031-62660-9_11.
7. Zhang T, Wu X, Pan Y, Luo D, Xu Y, Zhang Z, et al. Vibration energy harvesting system based on track energy-recycling technology for heavy-duty freight railroads. Appl Energy. 2022;323:119673. doi:10.1016/j.apenergy.2022.119673.
8. Shu C, Cao Y, Sun T, Zhang T, Wang X. Energy recovery in automotive systems: a review of regenerative braking, flywheel, thermoelectric, rankin cycle and electric turbo compound. Appl Comput Eng. 2024;85:44–60. doi:10.54254/2755-2721/85/20240623.
9. Sarker MT, Haram MHSM, Shern SJ, Ramasamy G, Al Farid F. Second-life electric vehicle batteries for home photovoltaic systems: transforming energy storage and sustainability. Energies. 2024;17(10):2345. doi:10.3390/en17102345.

10. Kong LB, Li T, Hng HH, Boey F, Zhang T, Li S. Waste energy harvesting. Lect Notes Energy. 2014;24:263–403. doi:10.1007/978-3-642-54634-1.
11. Pimenov DY, Mia M, Gupta MK, Machado Á.R, Pintaude G, Unune DR, et al. Resource saving by optimization and machining environments for sustainable manufacturing: a review and future prospects. Renew Sustain Energy Rev. 2022;166:112660. doi:10.1016/j.rser.2022.112660.
12. Haram MHSM, Sarker MT, Ramasamy G, Ngu EE. Second life EV batteries: technical evaluation, design framework, and case analysis. IEEE Access. 2023;11:138799–812. doi:10.1109/ACCESS.2023.3340044.
13. Zheng XF, Liu CX, Yan YY, Wang Q. A review of thermoelectrics research—recent developments and potentials for sustainable and renewable energy applications. Renew Sustain Energy Rev. 2014;32:486–503. doi:10.1016/j.rser.2013.12.053.
14. Onyeke FO, Odujobi O, Adikwu FE, Elete TY. Advancements in the integration and optimization of control systems: overcoming challenges in DCS, SIS, and PLC deployments for refinery automation. Open Access Res J Multidiscip Stud. 2022;4(2):94–101. doi:10.53022/oarjms.2022.4.2.0095.
15. Bai S, Liu C. Overview of energy harvesting and emission reduction technologies in hybrid electric vehicles. Renew Sustain Energy Rev. 2021;147:111188. doi:10.1016/j.rser.2021.111188.
16. Zhao W, Wu G, Wang C, Yu L, Li Y. Energy transfer and utilization efficiency of regenerative braking with hybrid energy storage system. J Power Sources. 2019;427:174–83. doi:10.1016/j.jpowsour.2019.04.083.
17. Tauseef SM, Abbasi T, Abbasi SA. Energy recovery from wastewaters with high-rate anaerobic digesters. Renew Sustain Energy Rev. 2013;19:704–41. doi:10.1016/j.rser.2012.11.056.
18. Bideris-Davos AA, Vovos PN. Comprehensive review for energy recovery technologies used in water distribution systems considering their performance, technical challenges, and economic viability. Water. 2024;16(15):2129–10. doi:10.1109/TIM.2023.3290297.
19. Zhao LC, Zou HX, Wei KX, Zhou SX, Meng G, Zhang WM. Mechanical intelligent energy harvesting: from methodology to applications. Adv Energy Mater. 2023;13(29):2300557. doi:10.1002/aenm.202300557.
20. Zhao LC, Zhou T, Chang SD, Zou HX, Gao QH, Wu ZY, et al. A disposable cup inspired smart floor for trajectory recognition and human-interactive sensing. Appl Energy. 2024;357:122524. doi:10.1016/j.apenergy.2023.122524.
21. Ahmed J, Salam Z. An improved perturb and observe (P&O) maximum power point tracking (MPPT) algorithm for higher efficiency. Appl Energy. 2015;150:97–108. doi:10.1016/j.apenergy.2015.04.006.
22. Kiran SR, Basha CH, Singh VP, Dhanamjayulu C, Prusty BR, Khan B. Reduced simulative performance analysis of variable step size ANN based MPPT techniques for partially shaded solar PV systems. IEEE Access. 2022;10:48875–89. doi:10.1109/ACCESS.2022.3172322.
23. Sakunthala S, Kiranmayi R, Mandadi PN. A review on speed control of permanent magnet synchronous motor drive using different control techniques. In: Proceedings of the 2018 International Conference on Power, Energy, Control and Transmission Systems (ICPECTS); 2018 Feb 22–23; Chennai, India.
24. Wang J, Wang D, Wang S, Tong T, Sun L, Li W, et al. A review of recent developments in permanent magnet eddy current couplers technology. Actuators. 2023;12(7):277. doi:10.3390/act12070277.
25. Li N, Xia H, Yang C, Luo T, Qin L. Investigation of a novel ultra-low-frequency rotational energy harvester based on a double-frequency up-conversion mechanism. Micromachines. 2023;14(8):1645. doi:10.3390/mi14081645.
26. Chen PY, Lee KY, Huang PC, Li JH, Chiu FC, Tsai JF, et al. The performance analysis of the low-speed direct-drive generators for harvesting current energy. IET Renew Power Gener. 2023;17(2):305–16. doi:10.1049/rpg2.12598.
27. Cao Z, Zhou H, Han C, Jing H, Wang ZL, Wu Z. High-performance rotating structure triboelectric-electromagnetic hybrid nanogenerator for environmental wind energy harvesting. ACS Appl Mater Interfaces. 2024;16(45):62254–63. doi:10.1021/acsami.4c15551.
28. He L, Han Y, Sun L, Wang H, Zhang Z, Cheng G. A rotating piezoelectric-electromagnetic hybrid harvester for water flow energy. Energy Convers Manage. 2023;290:117221. doi:10.1016/j.enconman.2023.117221.
29. Li J, Wang G, Yang P, Wen Y, Zhang L, Song R, et al. An orientation-adaptive electromagnetic energy harvester scavenging for wind-induced vibration. Energy. 2024;286:129578. doi:10.1016/j.energy.2023.129578.

30. Tripathi SM, Tiwari AN, Singh D. Grid-integrated permanent magnet synchronous generator-based wind energy conversion systems: a technology review. Renew Sustain Energy Rev. 2015;51:1288–305. doi:10.1016/j.rser.2015.06.060.
31. Yao G, Luo Z, Lu Z, Wang M, Shang J, Guerrerob JM. Unlocking the potential of wave energy conversion: a comprehensive evaluation of advanced maximum power point tracking techniques and hybrid strategies for sustainable energy harvesting. Renew Sustain Energy Rev. 2023;185:113599. doi:10.1016/j.rser.2023.113599.
32. Wei J, Sarker MT, Ramasamy G, Thiagarajah SP, Aman F. Industrial untapped rotational kinetic energy assessment for sustainable energy recycling. Energy Eng. 2025;122(3):905–27. doi:10.32604/ee.2025.058916.